Available online at www.sciencedirect.com

SCIENCE DIRECT®

Biochimica et Biophysica Acta 1607 (2003) 53–63

BIOCHIMICA ET BIOPHYSICA ACTA

BBA

www.bba-direct.com

Acquisition of photosynthetic capacity by a reaction centre that lacks the Q_A ubiquinone; possible insights into the evolution of reaction centres?

Marion C. Wakeham[a], Dmitrij Frolov[b], Paul K. Fyfe[a], Rienk van Grondelle[b], Michael R. Jones[a,*]

[a] *Department of Biochemistry, School of Medical Sciences, University of Bristol, University Walk, Bristol BS8 1TD, UK*

[b] *Department of Physics and Astronomy, Free University of Amsterdam, De Boelelaan 1081, 1081 HV, Amsterdam, The Netherlands*

Received 5 May 2003; received in revised form 8 August 2003; accepted 27 August 2003

Abstract

A photosynthetically impaired strain of *Rhodobacter sphaeroides* containing reaction centres with an alanine to tryptophan mutation at residue 260 of the M-polypeptide (AM260W) was incubated under photosynthetic growth conditions. This incubation produced photosynthetically competent strains containing suppressor mutations that changed residue M260 to glycine or cysteine. Spectroscopic analysis demonstrated that the loss of the Q_A ubiquinone seen in the original AM260W mutant was reversed in the suppressor mutants. In the mutant where Trp M260 was replaced by Cys, the rate of reduction of the Q_A ubiquinone by the adjacent (H_A) bacteriopheophytin was reduced by three-fold. The findings of the experiment are discussed in light of the X-ray crystal structures of the wild-type and AM260W reaction centres, and the possible implications for the evolution of reaction centres as bioenergetic complexes are considered.

Keywords: Reaction centre; *Rhodobacter sphaeroides*; Ubiquinone

1. Introduction

Photosynthetic reaction centres are responsible for the transduction of light energy into a biologically useful form. The last couple of years have seen significant advances in our understanding of the structure and design of reaction centres through the publication of a high-resolution structure of the Photosystem I complex from the thermophilic cyanobacterium *Synechococcus elongatus* [1,2], and the publication of lower resolution structures of the Photosystem II complex [3–7]. As this crystallographic information has emerged, it has reinforced the view that despite considerable differences in size and complexity, photosynthetic reaction centres have a common basic design, a common fundamental mechanism, and are likely to have a common evolutionary origin [8–14].

All reaction centres use light energy to change the redox potential of a particular (bacterio)chlorophyll ((B)Chl) redox centre that forms part of an electron transfer chain. This triggers the reduction of centres "downstream" in the chain, and the oxidation of centres "upstream" in the chain, promoting linear and/or cyclic electron transfer. In purple photosynthetic bacteria such as *Rhodobacter (Rb.) sphaeroides*, light energy is used to power a cycle of electron transfer reactions that is linked to proton translocation across a charge-impermeable membrane [15,16]. The reaction centre connects to the electrical circuitry of this cyclic system through the double reduction (and double protonation) of a dissociable ubiquinone, and the single electron oxidation of a *c*-type cytochrome that is free to diffuse in the periplasmic compartment.

In terms of enzymology the purple bacterial reaction centre is a light-driven cytochrome c_2/ubiquinone oxidoreductase, the two active sites of the enzyme being connected by an electron transfer chain consisting of bacteriochlorophyll (BChl), bacteriopheophytin (BPhe) and ubiquinone [16]. From the standpoint of energetics, the *Rb. sphaeroides* reaction centre can also be viewed as a redox pump, transferring electrons from the relatively oxidising potentials

Abbreviations: BChl, bacteriochlorophyll; (B)Chl, bacteriochlorophyll and/or chlorophyll; BPhe, bacteriopheophytin; Chl, chlorophyll; P, primary donor of electrons; P*, first singlet excited state of P; *Rb.*, *Rhodobacter*

* Corresponding author. Tel.: +44-117-9287571; fax: +44-117-9288274.

E-mail address: m.r.jones@bristol.ac.uk (M.R. Jones).

0005-2728/$ - see front matter © 2003 Elsevier B.V. All rights reserved.
doi:10.1016/j.bbabio.2003.08.008

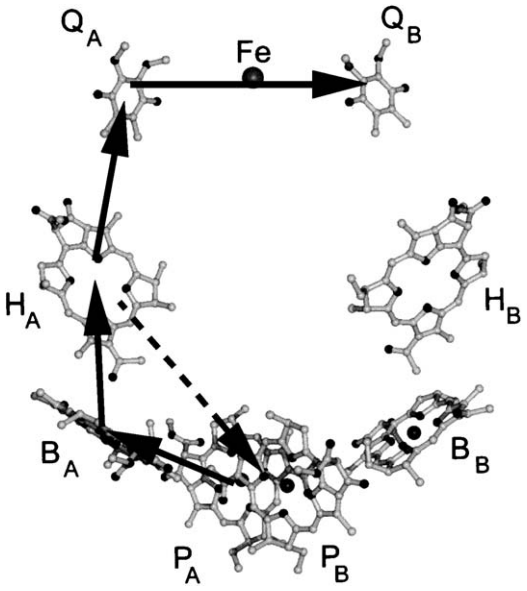

Fig. 1. Structure of the cofactors in the wild-type reaction centre. The black arrows show the route of light-driven electron transfer. The Q_A ubiquinone is not present in the AM260W mutant reaction centre, preventing forward electron transfer beyond the H_A BPhe and leading to recombination of the $P^+H_A^-$ radical pair (dotted arrow). The side-chains of the cofactors have been removed for clarity, and the reaction centre carotenoid is omitted. The figure was prepared using the programs Molscript [53] and Raster3D [54].

of the cytochrome c_2 Fe^{3+}/Fe^{2+} redox couple ($\sim +0.35$ V) to the relatively reducing potentials of the ubiquinone/ubiquinol redox couple ($\sim +0.09$ V) [17]. This transfer of electrons from oxidising to reducing redox potentials is a basic feature of reaction centre design. The key event in this is the absorption of light energy by a pair of BChl molecules that act as the primary donor of electrons (P); the formation of the first singlet excited state of P (denoted P*) alters the redox potential of the P BChls by some 1.4 V, transforming them into a powerful reductant.

Following excitation of the *Rb. sphaeroides* reaction centre by light, electrons are passed from the bacteriochlorin cofactors to the ubiquinone reductase (Q_B) site via a second, tightly bound ubiquinone (Q_A) (see Fig. 1). Previous experiments have shown that it is possible to exclude this ubiquinone from the complex by introducing an alanine to tryptophan mutation in the Q_A binding pocket, at the M260 position (AM260W) [18]. The resulting reaction centre lacks a cytochrome c_2/ubiquinone oxidoreductase activity, is blocked in transmembrane electron transfer beyond the BPhe electron acceptor (H_A; see Fig. 1), and is incapable of supporting photosynthetic growth of the organism [18]. Light energy absorbed by the BChls and BPhes of the complex is no longer used in a productive manner, and is dissipated either as heat or light (BChl fluorescence). X-ray crystallography of this AM260W mutant has shown that the mutation changes a small part of the protein structure such that the cavity which usually accommodates the head-group of the Q_A ubiquinone is no longer present [19]. This change in structure involves the conformation of a short loop of six amino acids that connects the surface DE α-helix of the M-polypeptide to the membrane-spanning E α-helix (Fig. 2). The remainder of the structure is essentially unaffected by the mutation [19].

In this work, we have examined whether strains of *Rb. sphaeroides* containing reaction centres with the AM260W mutation can regain the capacity for photosynthetic growth through spontaneous mutation. Following incubation under photosynthetic growth conditions, strains have been isolated that have replacement of the tryptophan at the M260 position with either glycine or cysteine. These findings are discussed in the context of the possible processes that led to the first involvement of (bacterio)chlorin-containing complexes in electron transfer-based energy metabolism, and the emergence of reaction centres as bioenergetic complexes.

2. Materials and methods

2.1. Bacterial strains, growth media and growth conditions

Construction of the AM260W mutation has been described previously [18]. For the generation of suppressor mutants, the strain of *Rb. sphaeroides* containing AM260W mutant reaction centres also contained the LH1 and LH2 antenna complexes. For all other experiments, the *Rb.*

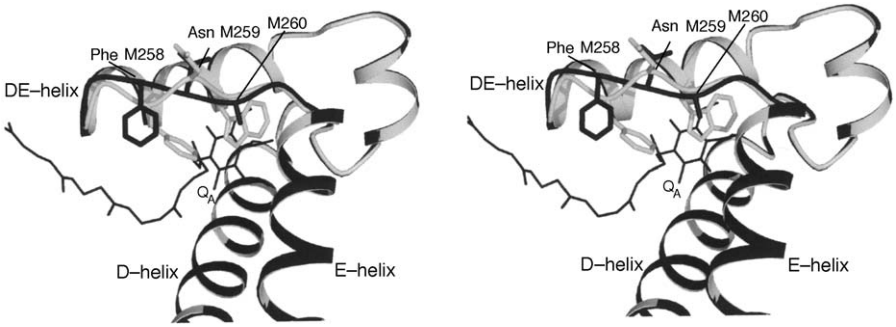

Fig. 2. Stereo-view of the change in structure induced by the AM260W mutation. The structure of the wild-type reaction centre (dark grey; [32]) was overlaid with that of the AM260W reaction centre (light grey; [19]) using the program LSQKAB [55]. The figure was prepared using the programs Molscript [53] and Raster3D [54], and the coordinate set 1QOV for the AM260W reaction centre [19].

sphaeroides strains used either contained reaction centres and the LH1 antenna complex, but lacked the LH2 antenna complex, or lacked both LH1 and LH2 (see below). A description of the genetic system used to achieve these combinations has been published previously [20].

Growth of *Rb. sphaeroides* under dark/semiaerobic conditions was carried out as described previously, using M22+ medium supplemented with the appropriate antibiotics [21]. Growth of *Rb. sphaeroides* under illuminated/anaerobic conditions was carried out using SuccC medium [22] without any antibiotic supplement. For growth on solid media, M22+ or SuccC growth medium was supplemented with 1.5% (w/v) agar. Illuminated/anaerobic growth was carried out using a Bugbox anaerobic growth chamber (Ruskinn Technology, UK) illuminated with two 500-W tungsten flood lamps suspended outside the front panel of the chamber.

Intracytoplasmic membranes were prepared from cells grown under dark/semiaerobic conditions using a French pressure cell, as described elsewhere [21].

2.2. Millisecond time-scale transient absorbance spectroscopy

Millisecond (ms) time-scale transient absorption was recorded using a single beam spectrophotometer of local design. Trains of saturating actinic flashes were provided by a xenon flash-lamp (15 μF capacitor at 1000 V; 6 μs half-peak width) that was filtered with RG625 glass filters. Two light pipes (1 cm diameter) were used to deliver the excitation flashes to both sides of the sample cuvette in order to provide uniform illumination. The weak monochromatic measuring beam was detected using a photomultiplier that was protected from the excitation light by OG515 and BG39 cut-off filters. The output from the photomultiplier was passed through a current/voltage amplifier that had a time constant of 300 μs, and was digitised using a Microlink transient recorder. Samples were housed in a glass cuvette with an optical path length of 1 cm. For the purposes of comparison of different samples, in all experiments intracytoplasmic membranes were diluted to a reaction centre concentration of 1 μM, using the reaction centre absorbance band at 802 nm and an extinction coefficient of 288 mM^{-1} cm^{-1} [23] The intracytoplasmic membranes used contained reaction centres and LH1 antenna complexes, but lacked the LH2 antenna.

2.3. Femtosecond time-scale absorbance difference spectroscopy

Femtosecond transient absorbance difference spectra were recorded using antenna-deficient membranes, and a spectrometer that has been described previously [24]. In brief, the output of Ti/Sapphire oscillator was amplified by means of chirped pulse amplification (Alpha-1000 US, B.M. Industries) generating 1 kHz, 795 nm, 60 fs pulses. The absorption of the sample was 0.6 OD mm^{-1} at 795 nm, and typically 20% of the reaction centres were excited. Transient absorption spectra were collected with probe and excitation beams oriented at the magic angle. The steady state absorption of the sample before and after measurements did not show any changes. Spectra were corrected for the white light group velocity dispersion and instrument response function, and fitted globally with four components using an irreversible sequential model as described previously [25].

2.4. Analysis of the structure of the Q_A binding pocket

To analyse the density of protein packing in the region surrounding the M260 residue, a sphere of atoms of 15 Å radius centred upon the C_α carbon of the M260 amino acid was defined in the structural models of both the wild-type and AM260W mutant reaction centre [19]. The spheres were then analysed using the programs VOLUME and AREAIMOL [26]. The output from these programs calculated the percentage of the sphere that was occupied by atoms of the protein or by cofactors, the remainder being attributable to intra-protein cavities.

The X-ray crystal structure of the wild-type reaction centre was used as the basis for modelling the structure of the AM260C revertant. The program Xfit [27] was used to convert the side-chain from an alanine to a cysteine residue. The cysteine was then rotated to determine whether it could adopt a position in which there were no steric clashes with adjacent atoms. The same analysis was also undertaken with Ser, Leu and Arg replacements at position M260.

3. Results and discussion

3.1. Generation of suppressor/reversion mutations

Strains of *Rb. sphaeroides* containing the AM260W reaction centre are incapable of growth under anaerobic conditions in the light [18]. To determine if such strains could regain the capacity for photosynthetic growth, experiments were carried out on a strain of *Rb. sphaeroides* that contained the AM260W reaction centre together with the LH1 and LH2 antenna complexes. In this strain, the genes encoding the LH2 antenna complex are located on the bacterial genome, whilst the genes encoding the LH1 antenna complex (*pufBA*) and the L- and (mutant) M-polypeptides (*pufLM*) are located on a plasmid that is a derivative of pRKEH10 [20].

This mutant *Rb. sphaeroides* strain was grown under dark/semiaerobic conditions in M22+ liquid medium. Cells from this culture were streaked onto plates of SuccC growth medium supplemented with 1.5% (w/v) agar, and the agar plates were incubated overnight in the dark at 34 °C before transfer to a photosynthetic growth cabinet (see Materials and methods). Growth of five individual colonies was

observed on these plates after approximately 4 weeks. These colonies were then streaked on M22+ agar plates that were incubated under dark/semiaerobic conditions, and cells from these streak plates were used for the preparation of glycerol stocks. All subsequent growth of these strains was carried out under dark/semiaerobic conditions to prevent the generation of additional mutations.

3.2. Identification of mutations

The pRKEH10-derived plasmids containing the *pufLM* genes were isolated from cells of each of the photosynthetically competent *Rb. sphaeroides* strains. The cells used were from a culture grown under dark/semiaerobic conditions, and the plasmid DNA was isolated by the alkaline lysis miniprep method. In each case, the plasmid was amplified in *Escherichia coli*, and a 1841bp *Xba*I–*Bam*HI restriction fragment encompassing the *pufLM* genes was shuttled into plasmid pUC19 to provide template for dideoxy DNA sequencing. In an initial screen, the *Xba*I–*Bam*HI restriction fragments originating from the five photosynthetic-competent strains were sequenced through a region centred on the M260 codon. This revealed that three of the strains had a TGG → GGG single nucleotide mutation at this codon, corresponding to a mutation of Trp M260 to Gly. The remaining two strains had a TGG → TGT single nucleotide mutation, corresponding to the mutation Trp M260 to Cys. Thus none of the mutations detected in the initial screen involved a reversion of the mutant TGG codon to the wild-type GGC, which would involve a two-nucleotide change.

One isolate with each change was selected for a more detailed study, and was allocated the name AM260(W → G) or AM260(W → C), respectively. The *pufLM* genes from these isolates were sequenced in full, and in both cases the single base change at the M260 codon was found to be the only mutation in either *pufL* or *pufM*.

3.3. Construction of RC/LH1-only and antenna-deficient strains

To prepare material for spectroscopic analysis, two types of bacterial strain were constructed. First, the pRKEH10-derived plasmids containing the AM260(W → G) and AM260(W → C) mutations were introduced into *Rb. sphaeroides* strain DD13 by conjugative transfer [20]. Transconjugant strains were selected as described previously [20]. These strains contained reaction centres and the LH1 antenna complex, but lacked the LH2 antenna (termed RC/LH1-only strains). Growth experiments showed that the reaction centres in these strains were capable of supporting photosynthetic growth (data not shown). Fig. 3 shows absorbance spectra of intracytoplasmic membranes prepared from these RC/LH1-only strains, compared to that of an RC/LH1-only strain containing wild-type reaction centres. The similarity in the ratio of the intensity of the LH1 absorbance band at 875 nm and the reaction centre absorbance band at 802 nm indicates that the expression level of the mutant reaction centres was similar to that of the wild-type complex.

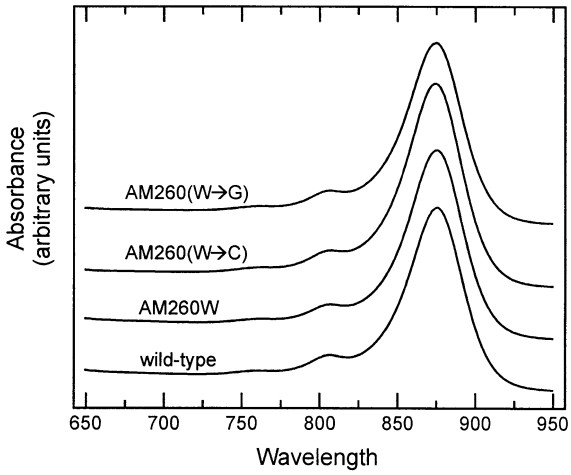

Fig. 3. Room temperature absorbance spectra of intracytoplasmic membranes prepared from strains with the LH1 antenna complex in addition to the (wild-type or mutant) reaction centre.

Second, antenna-deficient strains containing AM260 (W → G) and AM260(W → C) reaction centres were constructed. The 1841 bp *Xba*I–*Bam*HI restriction fragment encompassing the *pufL* and (mutant) *pufM* gene was excised from the pRKEH10-derived plasmids described above and transferred to plasmid pRKEH10D [20]. The latter is a derivative of plasmid pRKEH10 that lacks the *pufBA* genes that encode the LH1 antenna complex (due to a 300 bp deletion in *pufBA*). The pRKEH10D-derived plasmids containing the AM260(W → G) and AM260 (W → C) mutations were then introduced into *Rb. sphaeroides* strain DD13 by conjugative transfer [20]. The resulting transconjugant strains contained reaction centres but lacked both the LH1 and LH2 antenna. Absorbance spectra of intracytoplasmic membranes prepared from these antenna-deficient strains were identical to those from control antenna-deficient strains containing wild-type reaction centres (data not shown).

3.4. Restoration of Q_A function in the suppressor mutants

The acquisition of photosynthetic function in the AM260(W → C) and AM260(W → G) suppressor mutants implies restoration of a functional Q_A ubiquinone. Evidence that the Q_A ubiquinone was present in reaction centres from the suppressor mutants was provided by millisecond time-scale transient absorbance spectroscopy of intracytoplasmic membranes prepared from RC/LH1-only strains.

In the wild-type reaction centre, the radical pair states $P^+Q_A^-$ and/or $P^+Q_B^-$ are formed after photooxidation on a picosecond or microsecond time-scale, respectively. In the absence of a cytochrome donor to the reaction centre these states recombine to the neutral (PQ_AQ_B) state with time

constants of approximately 45 ms and 2 s, respectively, in membrane-bound reaction centres [28]. In the absence of forward electron transfer from the H_A BPhe to the Q_A ubiquinone, in a reaction centre where this quinone has been chemically reduced or extracted for example, electron or energy transfer events amongst the reaction centre bacteriochlorins take place on a sub-millisecond time-scale. The dominant process is recombination of the $P^+H_A^-$ radical pair (dotted arrow in Fig. 1), and this takes place on a time-scale of a few nanoseconds. The primary donor triplet excited state can also be formed in a subpopulation of reaction centres. This triplet has a lifetime of 30 ns or 50 μs, varying with the presence or absence of the reaction centre carotenoid. Given this, observation of photooxidation of P on a millisecond time-scale is therefore an indicator of electron transfer from P to the Q_A ubiquinone (and possibly on to the Q_B ubiquinone).

Fig. 4 shows P^+ formation in intracytoplasmic membranes containing reaction centres and the LH1 antenna, measured by monitoring the absorbance change at 542 nm elicited by flash excitation [29,30]. Difference transient absorbance measurements at 551 minus 542 nm showed that intracytoplasmic membranes prepared from strains with this LH2-deficient phenotype are deficient in cytochrome c_2 (data not shown). In membranes containing wild-type reaction centres, a train of 10 excitation pulses produced an absorbance change corresponding to the formation of the $P^+Q_A^-$ and/or $P^+Q_B^-$, the signal decaying between flashes.

The abrupt flash-induced absorbance changes seen for the wild-type reaction centre were not observed in measurements on membranes containing AM260W mutant reaction centres (Fig. 4), consistent with the absence of the Q_A ubiquinone in this mutant. However, there was a small absorbance increase that built gradually during the flash train, and decayed very slowly in the subsequent period. This signal is attributed to a small amount of direct formation of the $P^+Q_B^-$ state via electron transfer along the B-branch of cofactors, and is the subject of a recent report [31].

The results obtained for the reaction centres containing the suppressor mutations were similar to those obtained for the wild-type complex, showing the formation of the $P^+Q_A^-$/$P^+Q_B^-$ state in response to each excitation flash, with decay of this state in the dark period between flashes (Fig. 4). The simplest interpretation of this result is that the suppressor mutations restore the Q_A binding site, enabling formation of the long-lived $P^+Q_A^-$ and $P^+Q_B^-$ states.

3.5. Modelling of the Q_A binding pocket in the AM260 (W→C) mutant

In principle, a one nucleotide mutation of the codon TGG could give rise to codons for Arg (2), Gly, Ser, Leu, Cys (2) or a stop codon (2). The Cys and Gly that were actually generated are similar to the Ala that occurs at the M260 position in the wild-type reaction centre in that they are also relatively small amino acids. Presumably, therefore, the acquisition of photosynthetic function in these suppressor mutants involves a return of this part of the protein to a structure similar to that in the wild-type complex, allowing

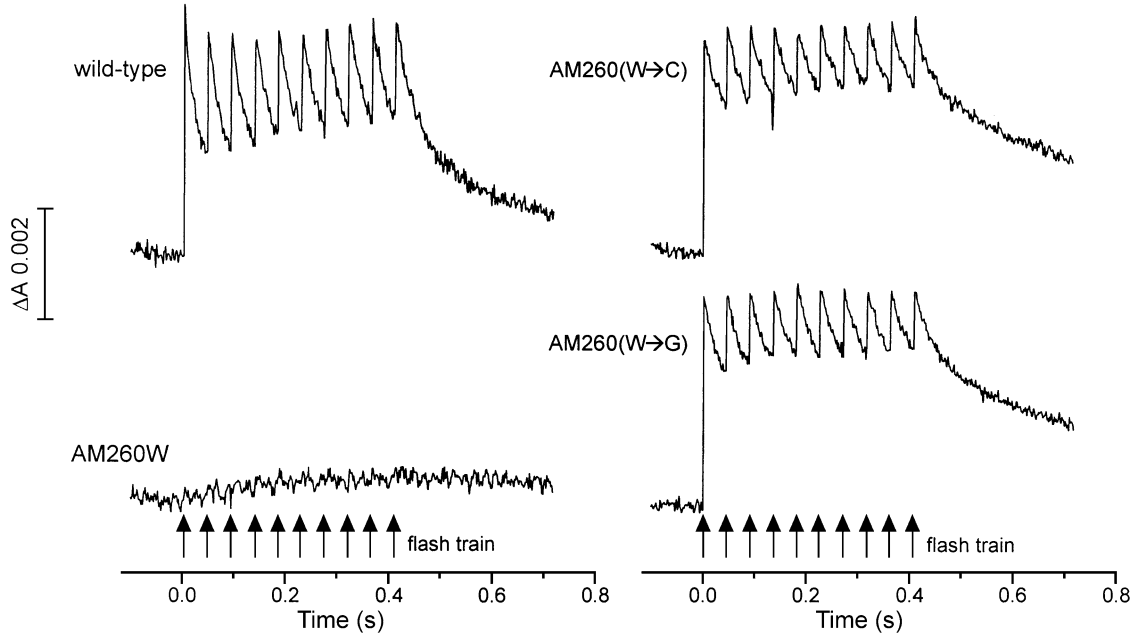

Fig. 4. Flash-induced absorbance changes associated with P photooxidation in intracytoplasmic membranes containing reaction centres and the LH1 antenna complex. The traces in Fig. 3 were normalised to the same concentration of reaction centres, using the absorbance band of the reaction centre at 802 nm (see Materials and methods). All samples were exposed to 10 excitation flashes delivered at 42 ms intervals. Data shown is an average of eight traces, collected at intervals of 30 s.

binding of the Q_A ubiquinone adjacent to a small M260 residue.

At this point, it is relevant to note that the AM260W mutation does not leave any large cavities in the protein interior, or produce a protein structure [19] that is obviously unstable or disordered (Fig. 2). To illustrate this, a sphere of 15 Å radius centred on the C_α carbon of the M260 amino acid was defined, and the partial volume occupied by atoms of the protein, cofactors or buried solvent molecules was calculated (see Materials and methods). The remainder of the sphere consists of intra-protein cavities. As can be seen from Table 1, application of this analysis to the X-ray crystal structure of the wild-type reaction centre [32] yielded a value of 82.4% for the protein (plus cofactor/solvent) content of this sphere, compared with a value of 80.3% calculated using the X-ray crystal structure of the AM260W reaction centre [19]. Thus the "density of packing" in this region of the protein complex is comparable in the two structures.

Also shown in Table 1 is the average crystallographic B-factor for the sphere of selected atoms expressed as a percentage of the average B-factor for the whole protein. Although the absolute values of the B-factors vary between the two structures, due to differences in data quality, when expressed in percentage terms the average B-factor for the selected region was comparable between the two structures (73.2% and 75.8%), indicating that relative mobility/disorder in the selected region was no greater in the AM260W mutant than in the wild-type complex. Looking more specifically at the disorder displayed by the residues that change conformation as a result of the AM260W mutation (see Fig. 2), the B-factors for the C_α carbon atoms of amino acids Trp/Ala M260, Asn M259 and Phe M258 were also comparable when expressed relative to the average B-factor for the whole protein (Table 1). The percentage values obtained for the C_α carbon atoms of Asn M259 and Phe M258 in the AM260W structure were a little higher than those obtained for the wild-type protein, but the actual B-factor was still lower than the average B-factor for the whole protein structure. The conclusion from this analysis is that the residues that undergo repacking are no more disordered or mobile in the new conformations they adopt in the AM260W reaction centre than in those they adopt in the wild-type complex.

Table 1
Analysis of protein structure adjacent to the M260 residue[a]

	Wild-type	AM260W
Volume of sphere (Å^3)	14,137	14,137
Volume occupied by protein (Å^3)	11,653	11,349
Percentage volume occupied by atoms	82.4%	80.3%
Average B-factor for all atoms in protein	59.4	39.2
Average B-factor for atoms in sphere	43.5	29.7
as percentage of average B-factor for all atoms	73.2%	75.8%
B-factor for C_α carbon of Ala/Trp M260	41.3	27.5
as percentage of average B-factor for all atoms	69.5%	70.2%
B-factor for C_α carbon of Asn M259	43.05	35.45
as percentage of average B-factor for all atoms	72.5%	90.4%
B-factor for C_α carbon of Phe M258	41.3	31.55
as percentage of average B-factor for all atoms	69.5%	80.5%

[a] Data were calculated as described in Materials and methods using the X-ray crystal structures of the wild-type [32] and AM260W [19] reaction centres.

Returning to the subject of the suppressor mutations, it is straightforward to suppose that Ala M260 could be replaced by a smaller Gly residue without affecting the structure of the Q_A binding pocket or the conformation of the Q_A ubiquinone. However, Cys is slightly larger than Ala, and so there is the question of whether this replacement would affect the structure of the Q_A site. To look at this, the structure of the wild-type reaction centre was used to model the replacement of Ala M260 by a Cys (see Materials and methods). In the wild-type complex, the bond connecting the C_α carbon of Ala M260 to the carbon of the side-chain methyl group is orientated approximately parallel to the plane of the ring of the Q_A ubiquinone, such that the methyl group sits over one face of the quinone ring (Fig. 5a). Modelling showed that this side-chain methyl could be replaced with the slightly larger Cys side-chain without causing a steric clash with any atoms of the ubiquinone head-group (Fig. 5b), or the surrounding protein. There was a small amount of overlap with one carbon atom of the isoprenoid side-chain of the ubiquinone (Fig. 5b), which in principle could be overcome by a minor repositioning of this part of the side-chain. Further modelling showed that this would also be the case for an Ala to Ser replacement at M260, which is another possible single nucleotide change for the TGG (Trp) codon (see above), but would not be the case for a Leu or Arg replacement at this position (data not shown).

3.6. Effects of a Cys residue at the M260 position on transmembrane electron transfer

To provide further evidence that Q_A function was restored in the AM260(W → C) mutant, and to look at the consequences of this buried Cys residue for transmembrane electron transfer, the kinetics of transmembrane electron transfer were investigated by picosecond time-scale transient absorbance spectroscopy of membrane-bound AM260 (W → C) reaction centres, as described in Materials and methods. The AM260(W → G) reaction centre was not investigated. In preliminary experiments, it was established that the room temperature and 77 K absorbance spectra of the membrane-bound AM260(W → C) reaction centre were identical to those of the wild-type membrane-bound reaction centre, as was the room temperature circular dichroism spectrum (data not shown).

Absorbance difference spectra were obtained at varying time intervals after a 795 nm excitation pulse, with a maximum delay time of 3.5 ns. Spectra recorded at several delay times are shown in Fig. 6. The 795 nm pulse mainly

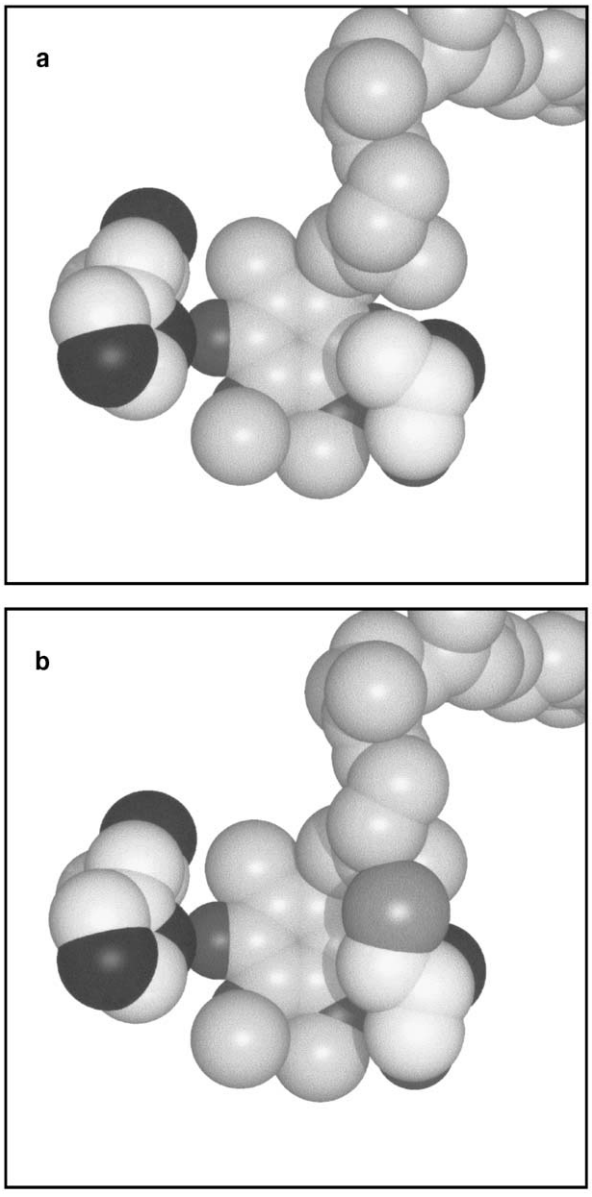

Fig. 5. Structure of the Q_A ubiquinone and the M260 residue in the wild-type reaction centre (a) and model of these groups in the AM260(W → C) reaction centre (b). Also shown is residue His M219, that provides a hydrogen bond to the C4 carbonyl group of the ubiquinone head-group. Modelling of a Cys at residue M260 was carried out as described in Materials and methods. Carbon atoms are shown in grey, nitrogen atoms in black, and the oxygen atoms of the ubiquinone head-group and sulfur atom of the Cys M260 side-chain (b) are shown in dark grey.

excited the B_A monomeric BChl, with some excitation of the B_B monomeric BChl, causing a bleach around 800 nm at early delay times (64 fs spectrum, Fig. 6). Subsequent rapid excitation transfer from the monomeric BChls to the P BChl dimer caused a bleaching of P band around 870 nm, concomitant with a loss of the bleach at 800 nm (0.5 ps spectrum, Fig. 6). Stimulated emission on the red side of the bleach of the 870 nm P band was maximal at around 0.5 ps, and subsequently decayed as electron transfer took place from P* to the H_A BPhe (33 ps spectrum compared with 0.5 ps spectrum, Fig. 6).

A global analysis of the data was carried out using an irreversible sequential model (i.e. $1 \rightarrow 2 \rightarrow 3 \rightarrow$). Four spectrally and temporally distinct components were needed to describe the data, and the Species Associated Difference Spectra (SADS) of these components are shown in Fig. 7. The first component was attributed to the short-lived excited states of the accessory BChls (B*), with a lifetime of 130 fs (Fig. 7a). This evolved into a state with a spectrum that was characteristic of P*, which in turn had a lifetime of 5.6 ps (Fig. 7b). This lifetime was a little longer than that usually described for purified wild-type reaction centres, but was similar to the 4.5–4.8 ps determined previously for membrane-bound wild-type *Rb. sphaeroides* reaction centres [33,34]. Given that it has been shown that electron transfer can also be driven by B_A^* in wild-type reaction centres [35], it is also possible that there was a contribution of a small amount of $P^+B_A^-$ and/or $B_A^+H_A^-$ to the spectrum in Fig. 7b.

The third state revealed by the analysis was assigned to $P^+H_A^-$ (Fig. 7c). Although this state had a spectrum that was similar to that determined previously for the membrane-bound wild-type reaction centre [34], it decayed with a lifetime (635 ps) that was significantly longer than that associated with this state in the wild-type complex (175–210 ps [33,34]). The final state (Fig. 7d) had the spectral features characteristic of $P^+Q_A^-$, and had a lifetime that was infinite on the time-scale of the measurement. Formation of this state was not observed during previous measurements on the Q_A-deficient AM260W reaction centre [18].

Based on these data, the main effect of the Cys residue at the M260 position was a three-fold slowing of the rate of electron transfer from $P^+H_A^-$ to $P^+Q_A^-$. Given the location of this Cys residue, on the opposite side of the ubiquinone head-group to the H_A BPhe, it seems likely that this slowing

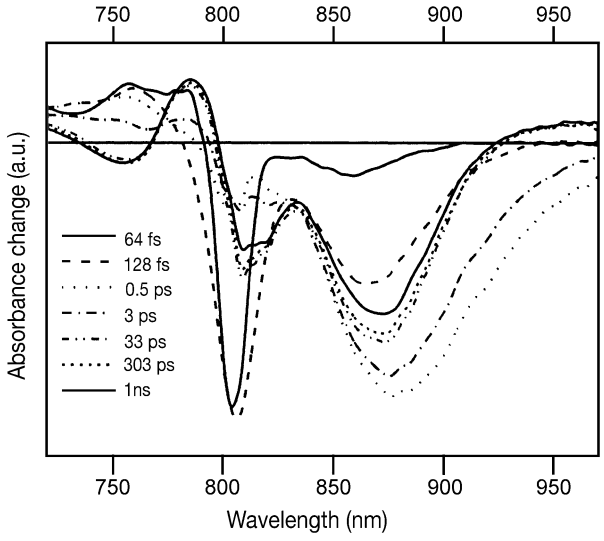

Fig. 6. Transient absorbance difference spectra obtained at various times after excitation of membrane-bound AM260(W → C) reaction centres with a 60 fs excitation pulse centred at 795 nm.

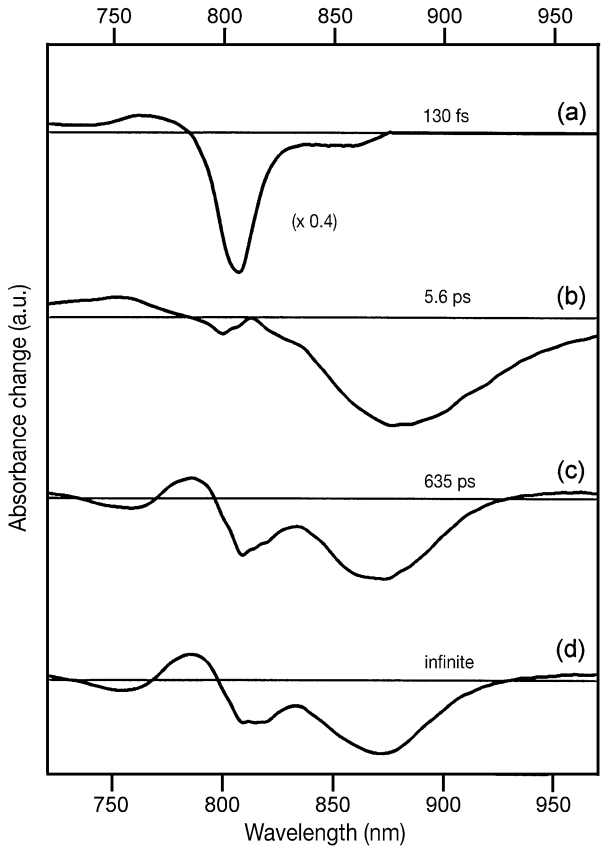

Fig. 7. SADS and associated lifetimes derived from a global analysis of transient absorbance spectra obtained after 795 nm excitation of membrane-bound AM260(W → C) reaction centres. For the purposes of comparison, spectrum (a) has been multiplied by a factor of 0.4.

was due to an effect on the driving force or reorganization energy for this reaction, rather than a change in the distance between the H_A and Q_A cofactors. It is possible to envisage that the electronegative Cys sulfur atom could affect redox potential of the Q_A ubiquinone, and/or that replacement of an apolar alanine with a polar Cys residue could affect the reorganization energy for Q_A reduction. Another possibility is that the strength of the hydrogen bond interaction between the C1 carbonyl group of the Q_A ubiquinone and the surrounding protein could be modified, as in the wild-type reaction centre this hydrogen bond is donated by the backbone amide group of the M260 amino acid.

3.7. Creation of a quinone binding site in a membrane-bound redox protein—a step in the evolution of the ancestral reaction centre?

The capacity of mutationally impaired *Rb. sphaeroides* reaction centres to regain full function through suppressor or reversion mutations is well documented [36–44], and so the generation of the AM260(W → C) and AM260(W → G) mutations following the application of photosynthetic selection pressure is not surprising. Perhaps the most interesting aspect of the experiments described above, or for that matter from the original Ala to Trp mutation when viewed in reverse, is that photosynthetic capacity is acquired by a non-functional complex as a result of the recruitment of a new cofactor (the Q_A ubiquinone), following a genetic change of only one or two nucleotides. This minor change in the sequence of the *pufM* gene radically alters the fate of light energy harvested by the BChls of the organism, enabling productive use of part of the absorbed energy through the generation of a protonmotive force and coupled ATP synthesis.

Looking at the AM260W reaction centre more closely, none of the light energy captured by the BChls of this complex is used in a productive manner. The absorbed energy is either lost as near-infrared fluorescence from the P* state, or as heat during a number of energy- or electron-transfer processes. These include internal conversion between different BChl-excited electronic states, excitation energy transfer between BChls (and BPhes), and through recombination of radical pairs such as $P^+H_A^-$ to the ground state. The AM260W reaction centre therefore acts as a dissipater of absorbed light energy, but is useless from the point of view of meeting the energy requirements of the cell.

These attributes, and failings, are reminiscent of those proposed for the forerunner of the ancestral reaction centre. The extant photosynthetic reaction centres are supported in their role by a series of enzymes that synthesise the Chl-type pigments. It has therefore been proposed that energy-transducing reaction centres may have evolved from Chl-containing proteins that had a different function. Larkum [45], and Mulkidjanian and Junge [46], have presented alternative scenarios in which reaction centres are proposed to have evolved from proteins whose primary function was to provide protection from photodamage by UV radiation. Chl and BChl are suitable as quenchers of potentially harmful UV photons due to their strong absorbance in the UV, through the Soret transition, and the photochemistry of the molecule in which energy is passed by internal conversion to the low energy Q_y transition in the red or near-infrared region of the spectrum. Mulkidjanian and Junge [46] developed a detailed model on how such a UV-protecting BChl protein would work, with clusters of aromatic amino acids contributing to the harvesting of UV photons, and passing the excited state energy on to BChls for dissipation as heat or, through fluorescence, as visible light. Interestingly, Lin et al. [47] have suggested that the B-branch BPhe (H_B) and accessory BChl (H_B) of the purple bacterial reaction centre have been retained during the course of evolution in order to fulfil such a photoprotective function, and have shown that electron transfer occurs among the B-branch bacteriochlorins following the absorption of photons of blue light (390 nm).

An attractive aspect of this hypothesis is that it gives a prominent role to the most distinctive feature of (B)Chl-type cofactors, their strong absorbance in the UV/visible range, and a later secondary role to their redox properties. However, although the origins of reaction centres as UV-protect-

ing membrane proteins is a thought-provoking idea, it should be noted that alternative suggestions have been made for the function of ancestral BChl-containing proteins [48], and it has also been proposed that Type II reaction centres are descended from the *b*-type cytochromes found in respiratory electron transfer chains [49,50].

In their evolutionary scenario, Mulkidjanian and Junge [46] proposed that the key step in the metamorphosis of a UV-protecting BChl protein into an energy-transducing BChl protein would be the occurrence of mutations that prevent the binding of one or more BChls. It was envisaged that this could result in a cavity in the protein, into which were bound redox cofactors such as quinones or iron–sulfur centres. The experiments described in this report point to a simpler alternative in which replacement of a bulky residue (Trp) by a small residue (Gly, Cys or Ala), in a suitable part of the protein, produces a small cavity that is capable of binding the head-group of a quinone. Presumably, for such a mutation to produce a quinone binding site during evolution would require a number of additional conditions to be met, such as accessibility of the cavity to quinone during assembly (for a "closed" site with tightly bound quinone like Q_A) or from the membrane phase (for an "open" site with transiently bound quinone like Q_B), and cavity-lining amino acids or backbone groups that are appropriate to binding of the quinone head-group. The acquisition of the sort of functionality seen at Q_B-type sites would likely require further mutations that facilitate the coupling of protonation to reduction (or deprotonation to oxidation for ubiquinol oxidase sites).

3.8. Characteristics of the "newly created" quinone binding site

The binding site of the Q_A ubiquinone in the wild-type *Rb. sphaeroides* reaction centre is formed by amino acids of the M-polypeptide, and Fig. 2 shows the backbone fold of the relevant region. The amino acids that form the binding site are located in the membrane-spanning D helix, the connecting DE helix, and a short loop from residue M256 to M261 that connects this DE helix to the membrane-spanning E helix. This loop connects two rigid elements of the protein structure (α-helices), and includes the M260 residue.

When the wild-type Ala M260 residue is mutated to Trp, removing part of the cavity that binds the Q_A quinone head-group, the M256–M261 loop undergoes a change in both backbone and side-chain structure in order to help fill the rest of the cavity [19]. Most noticeably, the side-chain of Phe M258 swings around to occupy space that is usually occupied by the tail of the Q_A ubiquinone (Fig. 2). As described above, the resulting structure is stable and well packed (Table 1).

Viewing this experiment in reverse, one could say that replacement of Trp M260 by Ala produces a cavity in the protein interior, and that the size of this cavity is increased by a change in the structure of the M256–M261 loop. As can be seen from Fig. 2, the creation of this cavity requires only modest changes in the structure of the protein, alterations in the backbone fold being accompanied by changes in the position of a number of side-chains, most noticeably Phe M258 and Asn M259. The result is a cavity that is matched to the size and shape of the quinone head-group, formed in an area of the protein that has some structural flexibility due to the presence of a loop in addition to α-helices. Located at one end of this cavity is a His residue (M219) that already donates a ligand to the non-heme iron, and is able to donate a hydrogen bond to one of the carbonyl groups of the ubiquinone head-group. The loop also folds in such a way that the backbone amide of residue M260 is able to form a hydrogen bond with the other ubiquinone carbonyl group. The reaction centre is therefore able to acquire a new cofactor with minimum disturbance to the main body of the complex, including the bundle of membrane-spanning α-helices and connecting amphipathic α-helices.

The structural flexibility associated with a loop region may also be extremely useful for tuning the redox potential of the quinone cofactor. As an illustration, Takahashi et al. [51,52] have described the properties of mutant reaction centres with Thr or Ser substitutions at residue Met M265 in the *Rb. sphaeroides* reaction centre. This residue forms part of the M256–M261 loop described above, and the Thr and Ser mutations produce decreases in the mid-point redox potential of the Q_A/Q_A^- couple of 100 and 85 mV, respectively [51]. In a recent manuscript, these changes in redox potential were attributed to a change in the conformation of the M256–M261 loop that weakens (lengthens) the hydrogen bond donated to the C1 carbonyl of the ubiquinone head-group by the backbone amide group of Ala M260 [52].

3.9. Consequences of the creation of a ubiquinone reductase site

In the experiments described above, replacement of Trp M260 by Gly, Cys or Ala creates a site in which ubiquinone can be reduced to the semiquinone, so facilitating the light-driven cycling of electrons from the high potential region of the bacterial electron transfer chain to the low potential region. The presence of the Q_A ubiquinone enables the reaction centre to deliver reducing equivalents to the ubiquinone pool, where electron flow is coupled to the translocation of protons across the membrane. The reaction centre is thus transformed from a complex that merely dissipates absorbed energy into one that can satisfy all of the energy requirements of the cell.

Although the initial effects may not have been so dramatic, it is possible to envisage that the recruitment of a quinone cofactor by the forerunner of the ancestral reaction centre could also have provided an opportunity for primitive electron transfer chains formed by the BChls of this progenitor complex to interface productively with the existing respiratory electron transfer system of the mem-

brane, and so contribute the energy requirements of the organism. A site at which quinone can be reduced to the semiquinone would not only provide a possible alternative route for the entry of reducing equivalents into the quinone pool, but also could have led to the stabilisation of charge-separated states within the reaction centre progenitor, producing longer lived BChl (or Chl) cations. As an illustration, the ~100 ms lifetime of the $P^+Q_A^-$ state formed in the wild-type complex is 10^7 longer than the ~10 ns lifetime of the $P^+H_A^-$ radical pair formed when Q_A is absent. Such a dramatic stabilisation of the charge-separated state could have had the knock-on effect of increasing the possibility of reduction of these (B)Chl cations by other high potential electron carriers, by making slow and inefficient electron donation by such centres competitive with slowed-down radical pair recombination inside the complex. Thus the binding of quinone would have opened up the possibility of both oxidation *and* reduction of the complex, introducing sunlight as a new energy source for the organism. As illustrated above, in principle this first step along the photosynthetic pathway could have been brought about by just one or two changes in the nucleotide sequence of the appropriate gene.

Acknowledgements

This work was supported by the Biotechnology and Biological Sciences Research Council of the United Kingdom and the University of Bristol (MCW, PKF and MRJ), and the Netherlands Organization for Scientific Research (NWO) via the Dutch Foundation for Earth and Life Sciences (ALW) (DF and RVG). The authors wish to thank Prof. Peter Rich from the Glynn Laboratory of Bioenergetics, University College London for the use of a kinetic spectrophotometer and helpful discussions, and Prof. Peter Heathcote of Queen Mary London for helpful discussions.

References

[1] P. Fromme, P. Jordan, N. Krauss, Structure of photosystem I, Biochim. Biophys. Acta 1507 (2001) 5–31.
[2] P. Jordan, P. Fromme, H.T. Witt, O. Klukas, W. Saenger, N. Krauss, Three-dimensional structure of cyanobacterial photosystem I at 2.5 Å resolution, Nature 411 (2001) 909–917.
[3] B. Hankamer, E.P. Morris, J. Barber, Revealing the structure of the oxygen-evolving core dimer of Photosystem-II by electron crystallography, Nat. Struct. Biol. 6 (1999) 560–564.
[4] J. Nield, E.V. Orlova, E.P. Morris, B. Gowen, M. van Heel, J. Barber, 3D map of the plant Photosystem-II supercomplex obtained by cryo-electron microscopy and single particle analysis, Nat. Struct. Biol. 7 (2000) 44–47.
[5] J.-R. Shen, N. Kamiya, Crystallization and the crystal properties of the oxygen-evolving photosystem II from *Synechococcus vulcanus*, Biochemistry 39 (2000) 14739–14744.
[6] A. Zouni, H.T. Witt, J. Kern, P. Fromme, N. Krauss, W. Saenger, P. Orth, First Photosystem-II crystals capable of water oxidation, Nature 409 (2001) 739–743.
[7] N. Kamiya, J.-R. Shen, Crystal structure of oxygen-evolving photosystem II from *Thermosynechococcus vulcanus* at 3.7-angstrom resolution, Proc. Natl. Acad. Sci. U. S. A. 100 (2003) 98–103.
[8] J. Barber, Photosynthetic reaction centers—a common link, Trends Biochem. Sci. 12 (1987) 321–326.
[9] H. Michel, J. Deisenhofer, Relevance of the photosynthetic reaction center from purple bacteria to the structure of Photosystem-II, Biochemistry 27 (1988) 1–7.
[10] W. Nitschke, A.W. Rutherford, Photosynthetic reaction centres: variations on a common structural theme, Trends Biochem. Sci. 16 (1991) 241–245.
[11] R.E. Blankenship, Origin and early evolution of photosynthesis, Photosynth. Res. 33 (1992) 91–111.
[12] P. Fromme, H.T. Witt, W.D. Schubert, O. Klukas, W. Saenger, N. Krauss, Structure of Photosystem-I at 4.5 Å resolution: a short review including evolutionary aspects, Biochim. Biophys. Acta 1275 (1996) 76–83.
[13] W.D. Schubert, O. Klukas, W. Saenger, H.T. Witt, P. Fromme, N. Krauss, A common ancestor for oxygenic and anoxygenic photosynthetic systems: a comparison based on the structural model of Photosystem-I, J. Mol. Biol. 280 (1998) 297–314.
[14] P. Heathcote, P.K. Fyfe, M.R. Jones, Reaction centres: structure and mechanism in biological solar power, Trends Biochem. Sci. 27 (2002) 79–87.
[15] A.J. Hoff, J. Deisenhofer, Photophysics of photosynthesis: structure and spectroscopy of reaction centres of purple bacteria, Phys. Rep. 287 (1997) 1–247.
[16] M.E. van Brederode, M.R. Jones, Reaction Centres of Purple Bacteria, in: N.S. Scrutton, A. Holzenburg (Eds.), Enzyme-Catalysed Electron and Radical Transfer, Kluwer Academic/Plenum Publishers, New York, USA, 2000, pp. 621–676.
[17] K.-I. Takamiya, P.L. Dutton, Ubiquinone in *Rhodopseudomonas sphaeroides*. Some thermodynamic properties, Biochim. Biophys. Acta 546 (1979) 1–16.
[18] J.P. Ridge, M.E. van Brederode, M.G. Goodwin, R. van Grondelle, M.R. Jones, Mutations that modify or exclude binding of the Q_A ubiquinone and carotenoid in the reaction center from *Rhodobacter sphaeroides*, Photosynth. Res. 59 (1999) 9–26.
[19] K.E. McAuley, P.K. Fyfe, J.P. Ridge, R.J. Cogdell, N.W. Isaacs, M.R. Jones, Ubiquinone binding, ubiquinone exclusion, and detailed cofactor conformation in a mutant bacterial reaction center, Biochemistry 39 (2000) 15032–15043.
[20] M.R. Jones, G.J.S. Fowler, L.C.D. Gibson, G.G. Grief, J.D. Olsen, W. Crielaard, C.N. Hunter, Construction of mutants of *Rhodobacter sphaeroides* lacking one or more pigment–protein complexes and complementation with reaction-centre, LH1, and LH2 genes, Mol. Microbiol. 6 (1992) 1173–1184.
[21] M.R. Jones, M. Heer-Dawson, T.A. Mattioli, C.N. Hunter, B. Robert, Site-specific mutagenesis of the reaction centre from *Rhodobacter sphaeroides* studied by Fourier transform Raman spectroscopy: mutations at tyrosine M210 do not affect the electronic structure of the primary donor, FEBS Lett. 339 (1994) 18–24.
[22] S.K. Bose, Media for anaerobic growth of photosynthetic bacteria, in: H. Gest, A. San Pietro, L.P. Vernon (Eds.), Bacterial Photosynthesis, Antioch Press, Yellow Springs, OH, 1963, pp. 501–510.
[23] S.C. Straley, W.W. Parson, D.C. Mauzerall, R.K. Clayton, Pigment content and molar extinction coefficients of photochemical reaction centers from *Rhodopseudomonas spheroides*, Biochim. Biophys. Acta 305 (1973) 597–609.
[24] C.C. Gradinaru, I.H.M. van Stokkum, A.A. Pascal, R. van Grondelle, H. van Amerongen, Identifying the pathways of energy transfer between carotenoids and chlorophylls in LHCII and CP29. A multicolor, femtosecond pump-probe study, J. Phys. Chem., B 104 (2000) 9330–9342.
[25] I.H.M. van Stokkum, T. Scherer, A.M. Brouwer, J.W. Verhoeven, Conformational dynamics of flexibly and semirigidly bridged electron

donor–acceptor systems as revealed by spectrotemporal parametrization of fluorescence, J. Phys. Chem. 98 (1994) 852–866.
[26] Collaborative Computational Project, Number 4, The CCP4 suite: programs for protein crystallography, Acta Crystallogr., D 50 (1994) 760–763.
[27] D.E. McRee, XtalView: a visual protein crystallographic software system for XII/Xview, J. Mol. Graph. 10 (1992) 44–46.
[28] R.R. Stein, A.L. Castellvi, J.P. Bogacz, C.A. Wraight, Herbicide-quinone competition in the acceptor complex of photosynthetic reaction centers from *Rhodopseudomonas sphaeroides*: a bacterial model for PS-II-herbicide activity in plants, J. Cell. Biochem. 24 (1984) 243–259.
[29] W.W. Parson, R.J. Cogdell, The primary photochemical reaction of bacterial photosynthesis, Biochim. Biophys. Acta 416 (1975) 105–149.
[30] W.W. Parson, R.K. Clayton, R.J. Cogdell, Excited states of photosynthetic reaction centers at low redox potentials, Biochim. Biophys. Acta 387 (1975) 265–278.
[31] M.C. Wakeham, M.G. Goodwin, C. McKibbin, M.R. Jones, Photoaccumulation of the $P^+Q_B^-$ radical pair state in purple bacterial reaction centres that lack the Q_A ubiquinone, FEBS Lett. 540 (2003) 234–240.
[32] K.E. McAuley-Hecht, P.K. Fyfe, J.P. Ridge, S.M. Prince, C.N. Hunter, N.W. Isaacs, R.J. Cogdell, M.R. Jones, Structural studies of wild type and mutant reaction centres from an antenna-deficient strain of *Rhodobacter sphaeroides*: monitoring the optical properties of the complex from cell to crystal, Biochemistry 37 (1998) 4740–4750.
[33] L.M.P. Beekman, R.W. Visschers, R. Monshouwer, M. Heer-Dawson, T.A. Mattioli, P. McGlynn, C.N. Hunter, B. Robert, I.H.M. van Stokkum, R. van Grondelle, M.R. Jones, Time-resolved and steady-state spectroscopic analysis of membrane-bound reaction centers from *Rhodobacter sphaeroides*: comparisons with detergent-solubilized complexes, Biochemistry 34 (1995) 14712–14721.
[34] L.M.P. Beekman, I.H.M. van Stokkum, R. Monshouwer, A.J. Rijnders, P. McGlynn, R.W. Visschers, M.R. Jones, R. van Grondelle, Primary electron transfer in membrane-bound reaction centers with mutations at the M210 position, J. Phys. Chem. 100 (1996) 7256–7268.
[35] M.E. van Brederode, F. van Mourik, I.H.M. van Stokkum, M.R. Jones, R. van Grondelle, Multiple pathways for ultrafast transduction of light energy in the photosynthetic reaction center of *Rhodobacter sphaeroides*, Proc. Natl. Acad. Sci. U. S. A. 96 (1999) 2054–2059.
[36] W.J. Coleman, D.C. Youvan, Spectroscopic analysis of genetically-modified photosynthetic reaction centers, Nature 366 (1993) 517–518.
[37] D.K. Hanson, D.M. Tiede, S.L. Nance, C.-H. Chang, M. Schiffer, Site-specific and compensatory mutations imply unexpected pathways for proton delivery to the Q_B binding-site of the photosynthetic reaction-center, Proc. Natl. Acad. Sci. U. S. A. 90 (1993) 8929–8933.
[38] S.H. Rongey, M.L. Paddock, G. Feher, M.Y. Okamura, Pathway of proton-transfer in bacterial reaction centers—2nd-site mutation Asn-M44 → Asp restores electron and proton-transfer in reaction centers from the photosynthetically deficient Asp-L213 → Asn mutant of *Rhodobacter sphaeroides*, Proc. Natl. Acad. Sci. U. S. A. 90 (1993) 1325–1329.
[39] M. Schiffer, C.F. Ainsworth, Y.-L. Deng, G. Johnson, F.H. Pascoe, D.K. Hanson, Proline in a transmembrane helix compensates for cavities in the photosynthetic reaction-center, J. Mol. Biol. 252 (1995) 472–482.
[40] A.K.W. Taguchi, J.E. Eastman, D.M. Gallo, E. Sheagley, W. Xiao, N.W. Woodbury, Asymmetry requirements in the photosynthetic reaction center of *Rhodobacter capsulatus*, Biochemistry 35 (1996) 3175–3186.
[41] D.K. Hanson, M. Schiffer, Symmetry-related mutants in the quinone binding sites of the bacterial reaction center—the effects of changes in charge distribution, Photosynth. Res. 55 (1998) 275–280.
[42] M.L. Paddock, M.E. Senft, M.S. Graige, S.H. Rongey, T. Turanchik, G. Feher, M.Y. Okamura, Characterization of second site mutations show that fast proton transfer to Q_B^- is restored in bacterial reaction centers of *Rhodobacter sphaeroides* containing the Asp-L213 → Asn lesion, Photosynth. Res. 55 (1998) 281–291.
[43] M. Valerio-Lepiniec, J. Miksovska, M. Schiffer, D.K. Hanson, P. Sebban, Mutations in the environment of the primary quinone facilitate proton delivery to the secondary quinone in bacterial photosynthetic reaction centers, Biochemistry 38 (1999) 390–398.
[44] J. Li, W.J. Coleman, D.C. Youvan, M.R. Gunner, Characterization of a symmetrized mutant RC with 42 residues from the Q_A site replacing residues in the Q_B site, Photosynth. Res. 64 (2000) 41–52.
[45] A.W.D. Larkum, The evolution of chlorophylls, in: H. Scheer (Ed.), Chlorophylls, CRC Press, Boston, 1991, pp. 367–383.
[46] A.Y. Mulkidjanian, W. Junge, On the origin of photosynthesis as inferred from sequence analysis, Photosynth. Res. 51 (1997) 27–42.
[47] S. Lin, E. Katilius, A.L.M. Haffa, A.K.W. Taguchi, N.W. Woodbury, Blue light drives B-side electron transfer in bacterial photosynthetic reaction centers, Biochemistry 40 (2001) 13767–13773.
[48] E.G. Nisbet, J.R. Cann, C.L. van Dover, Origins of photosynthesis, Nature 373 (1995) 479–480.
[49] T.E. Meyer, Evolution of photosynthetic reaction centers and light-harvesting chlorophyll proteins, Biosystems 33 (1994) 167–175.
[50] J. Xiong, C.E. Bauer, A cytochrome *b* origin of photosynthetic reaction centers: an evolutionary link between respiration and photosynthesis, J. Mol. Biol. 322 (2002) 1025–1037.
[51] E. Takahashi, T.A. Wells, C.A. Wraight, Protein control of the redox potential of the primary quinone acceptor in reaction centers from *Rhodobacter sphaeroides*, Biochemistry 40 (2001) 1020–1028.
[52] T.A. Wells, E. Takahashi, C.A. Wraight, Primary quinone (Q_A) binding site of bacterial photosynthetic reaction centers: mutations at residue M265 probed by FTIR spectroscopy, Biochemistry 42 (2003) 4064–4074.
[53] P.J. Kraulis, MOLSCRIPT—a program to produce both detailed and schematic plots of protein structures, J. Appl. Crystallogr. 24 (1991) 946–950.
[54] E.A. Merritt, D.J. Bacon, Raster3D: photorealistic molecular graphics, Methods Enzymol. 277 (1997) 505–524.
[55] W. Kabsch, A solution for the best rotation to relate two sets of vectors, Acta Crystallogr., A 32 (1976) 922–923.